1.1. Project details

Project title	Active filter functionalities for power converters in wind power plants
Project identification (program abbrev. and file)	12188
Name of the programme which has funded the project	FORSKEL
Project managing company/institution (name and address)	Aalborg University
Project partners	Aalborg University, Dong Energy Wind Power, ABB AB, Vestas Wind Systems A/S
CVR (central business register)	29 10 23 84
Date for submission	

1.2. Short description of project objective and results

The purpose of the project is to analyse and develop advanced Active Filter (AF) solutions based on implementation at the STATCOM level present in the WPP. Emphasis is given to make the AF efficient and stable during the continuously changing scenario of the network harmonic composition and WPP transients. Initially the possibility to consider hybrid AF was examined but it was agreed to drop the passive filtering part for economic reasons. Also, it was agreed to drop the AF at WT level as the focus is on AF at PCC.

The expected results are in the form of new AF control strategies possible to implement at the STATCOM level. The methods are developed and tested with in simulation considering Anholt WPP as a test-bench with the addition of the STATCOM at a 220 kV terminal in the WPP and voltage harmonics control at the 400 kV terminal in the grid according to specified harmonic limits. The strategies have to be validated experimentally using RTDS environment.

1.3. Executive summary

The project succeeded in solving the following main challenges:

- FDNE grid models in PSCAD and RSCAD to replicate realistic grid impedance scan data.
- Analysis and implementation of harmonic compensation by emulation of resistive behaviour at the selected harmonic frequencies.

- Development of novel voltage and current feedback AF strategy to be implemented in a remote connected STATCOM able to attenuate the harmonics amplification due to WPP or reduce the harmonics level to a lower limit without the need of grid impedance knowledge.

- The methods have been compared in terms of:

    - Total compensation current (RMS) for same attenuation to the background level

    - Ability to reduce the harmonics at T1 to lower levels and effect on down-stream busbars (T3, T4 and T5)

    - Efficient compensation and stable operation for

- The stability of the methods has been verified by RTDS and it was demonstrated for 16 different cases of grid impedance profile (the remaining 8 cases were not successfully represented as FDNE and we could not simulate them)

The following challenges remain still unsolved and could be considered as future work:

- Complete stability analysis theory (the difficulty is that the grid impedance is a very non-linear system with variable parameters)

- Improved FDNE modelling

The obtained results can be used by partners as new AF strategies to be implemented in real plants.

1.4. Project objectives

- Test benchmark model of the WPP

- Active filtering strategies STATCOM in WPP

- Implementation of active filtering at STATCOM level

- Demonstration on RTDS

1.5. Project results and dissemination of results

1.1.1 Plant description

Anholt offshore wind power plant (Fig. 1) is used here as the reference for developing the benchmark WPP model. The key details are:

- 400 MW offshore wind power plant comprising of 111 SWT-3.6-120 WTGs.
- Connected to the 400 kV grid at the onshore substation at Trige via two units of 400/220 kV, 450 MVA auto-transformers.
- 58 km aluminum 3x1x2000 mm^2 , 220 kV underground cable
- 24.5 km 3x1600 mm^2 220 kV sub-marine cable.
- 4x60 MVAr reactors at 220kV onshore transformer terminals
- 2x60 MVAr reactors at the 220 kV terminal between the onshore and offshore cable sections.
- 3x140 MVA, 220/33 kV plant step-up transformers.
- The collector grid has a total cable length of 152 km at 33 kV. The equivalent cable capacitance is 42 uF.

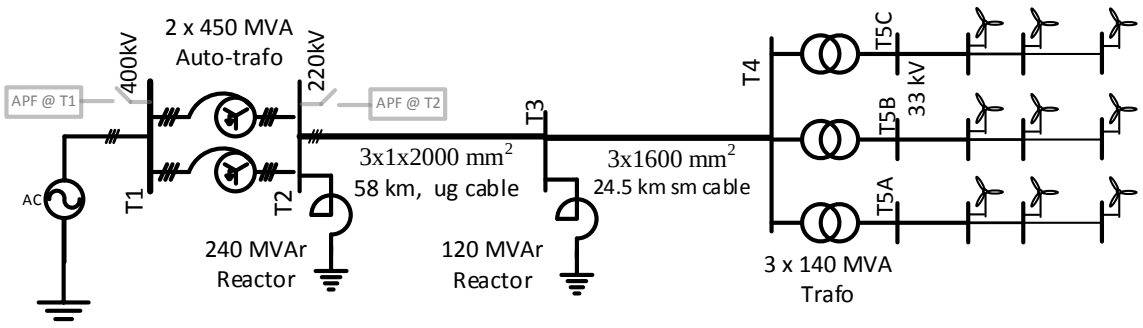

Fig. 1. WPP electrical network model.

The partners provided 24 sets of grid impedance vs frequency characteristics. These were modelled using the frequency dependent network equivalent (FDNE) components.

1.1.1.1 Background voltage harmonics in the grid model

The grid is represented by a Thevenin's equivalent voltage source with a frequency dependent series impedance. In DigSILENT, the background harmonic data can be entered in the form of a data table. In PSCAD and RSCAD, these have to be put in FORTRAN and C-Files respectively. The phase angles of the individual harmonic component and phase is assigned such that the different harmonic orders appear as positive, negative or zero sequence components.

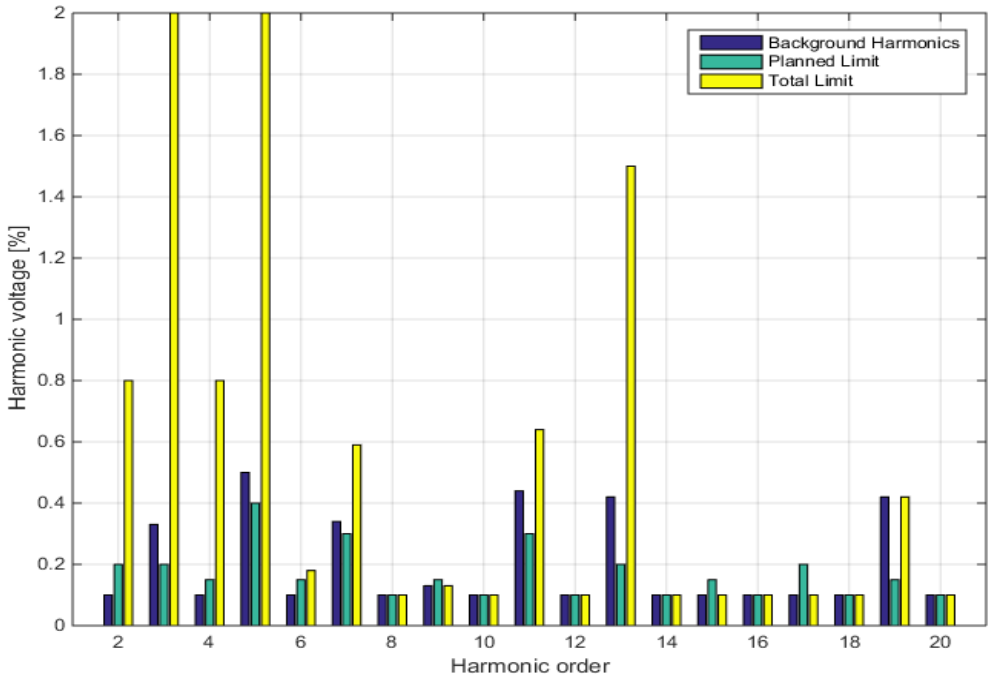

Fig. 2. Different target harmonic level: Background (Blue), recommended (Yellow) and planned (Green)

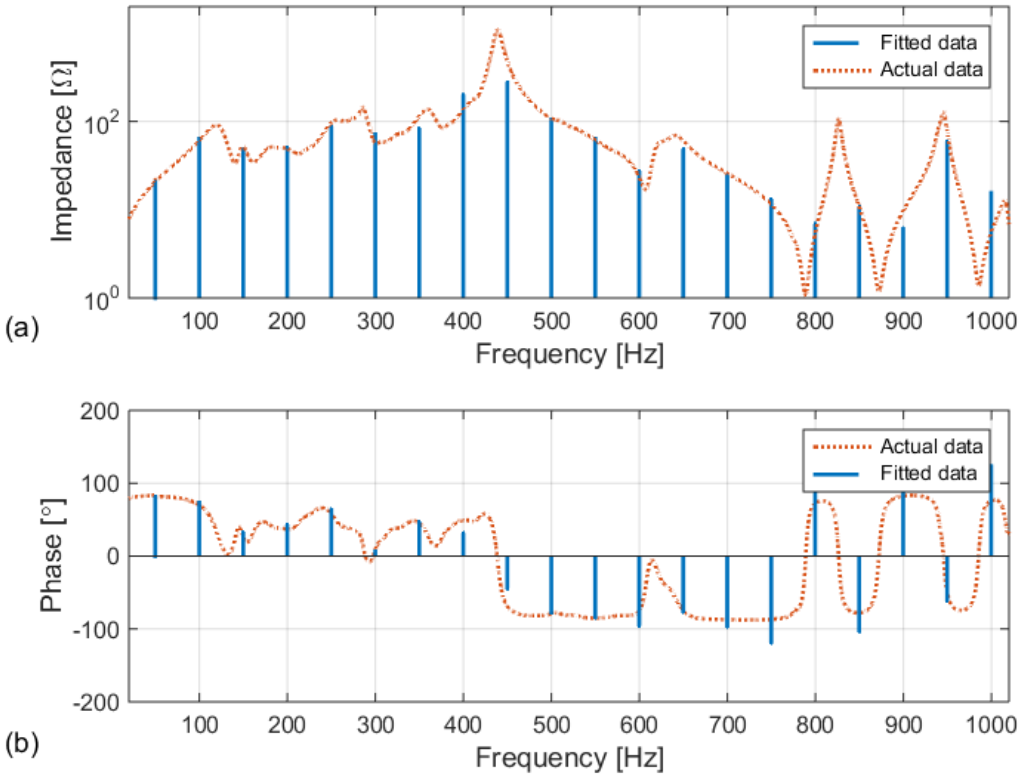

Fig. 3. Vector fitting of the impedance data. The continuous curve represents the input data, and the discrete stems indicate the impedance values at different harmonic orders.

1.1.1.2 Frequency dependent network equivalent (FDNE) for the grid impedance

In DigSILENT, the grid impedance data can be entered as a table of impedance values against frequency. However, in PSCAD and RSCAD, the impedance vs. frequency characteristics has to be converted into a transfer function using the curve-fitting algorithm developed by SINTEF[**]. It gives the A, B, C and D parameters of the frequency dependent admittance characteristics which can be simulated in PSCAD and RSCAD using FORTRAN or C –scripts. Recently PSCAD has introduced library component models to simulate these A, B, C, D model of the frequency dependent admittance, and this component has been used in this project. RSCAD has introduced a module which provides the curve fitting and generates the FDNE component. Fig. 3 gives the results of vector fitting of the grid admittance data. The grid admittance data in the range from 10 Hz to 1504.5 Hz was fitted with a 24th order transfer function which gave the fitting error of 0.67%. In RSCAD vector fitting program, all the data points (from 10 to 3000 Hz) was used.

1.1.2 WPP modelling

1.1.2.1 WTG

Type 4 wind turbines are considered in this project. Therefore, only the grid side converter has been modelled in terms of the average model. The dc link capacitor of 72mF has been modelled, which corresponds to a time constant of 11 ms at 1.05 kV dc link voltage reference. The model is shown in Fig. 4.

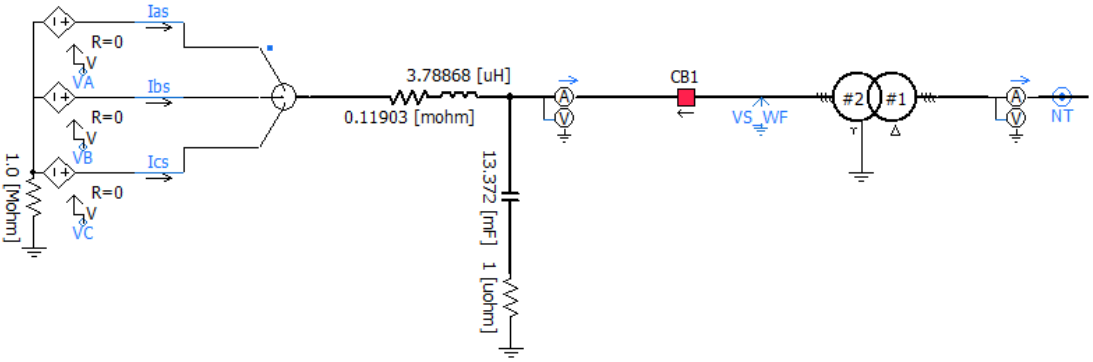

(a) Average model of the wind turbine grid side converter

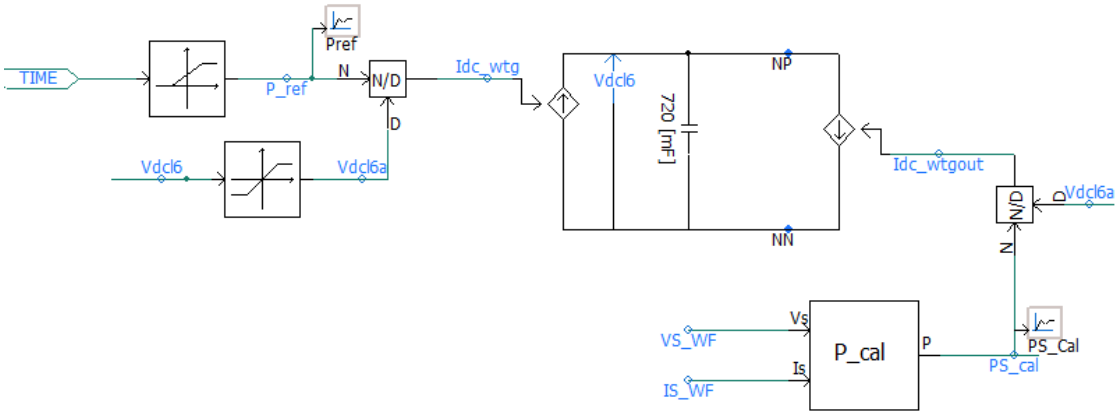

(b) DC link capacitor model.

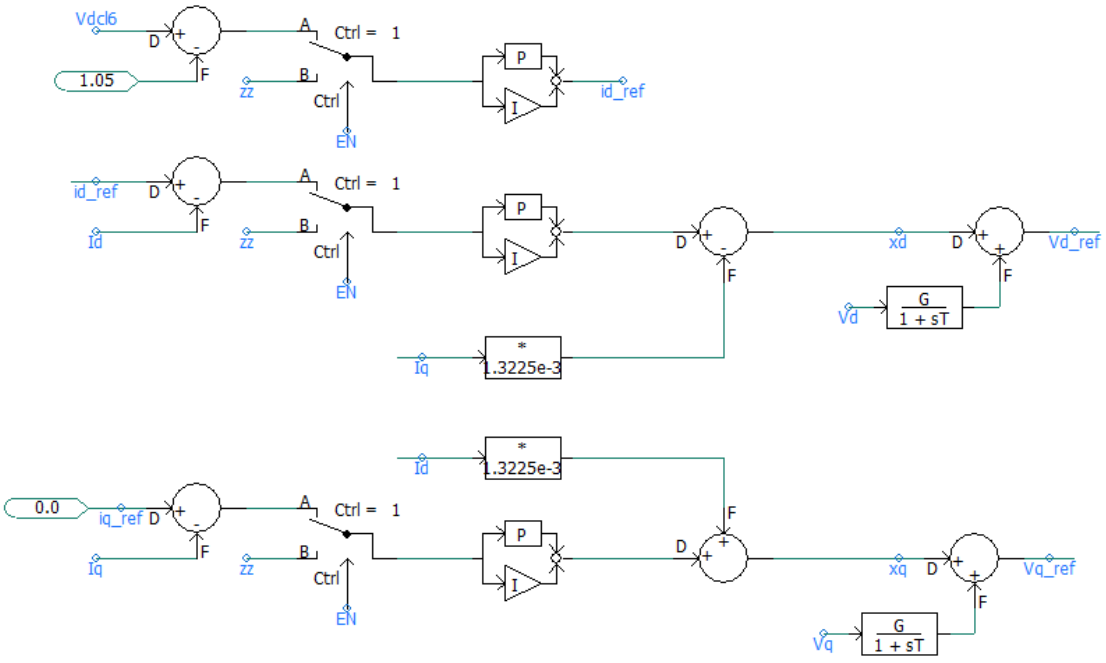

(c) Current control of the grid side converter

Fig. 4 Wind turbine model

1.1.2.2 WPP collection system and Transients in the collection system

As shown in Fig. 5. WPP model for transient simulation in PSCAD., the WPP collector system comprises three 140-MVA, 225/32 kV plant step-up transformers which connects the three collector feeders to the 220-kV bus T4. Each of the 33-kV feeder has 37x3.6 MW WT connected to it. In this simulation, the WTs on each feeder are grouped into three units of

10x3.6-MW and a 7x3.6-MW unit. The power order to these units are given from the control panel by the sliders, P10 and P7 respectively. The control panel also controls the circuit breakers in each feeders. The circuit breakers are included in this simulation so that the individual feeders can be connected7disconnected to create the transients in the WPP network.

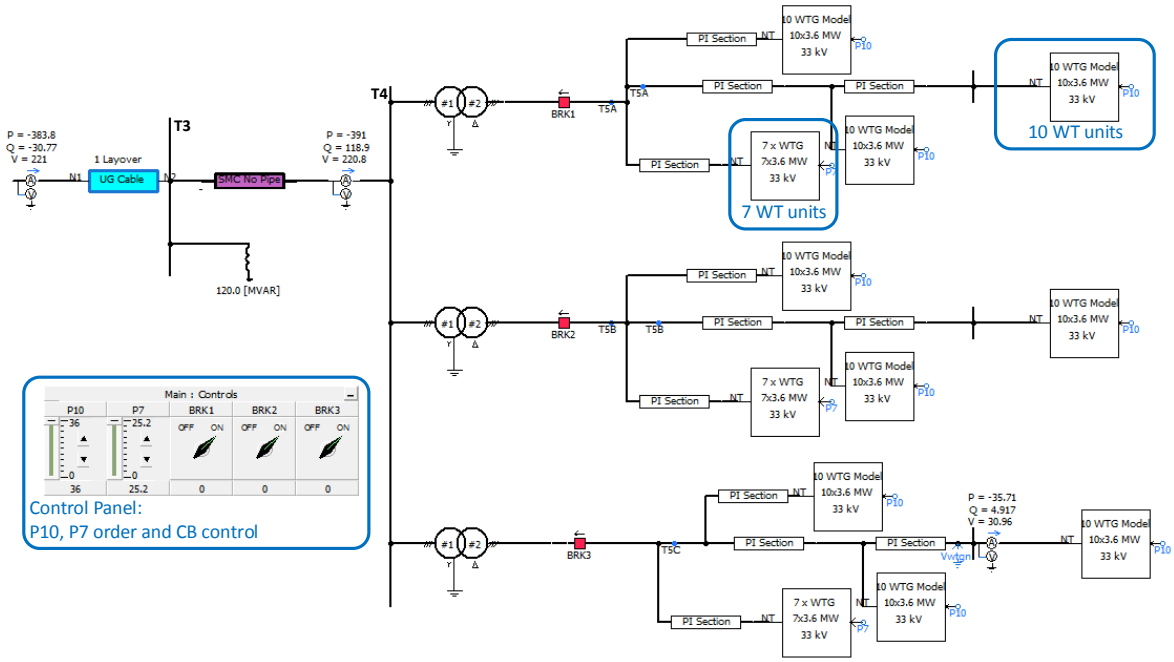

Fig. 5. WPP model for transient simulation in PSCAD.

1.1.2.3 Export cables

1.1.2.3.1 Underground Cable

The 58 km underground cable is laid in flat formation. Hence initially it was modelled in flat formation as shown in, using cable data from **Error! Reference source not found.**. A single layover section has been modelled as shown in **Error! Reference source not found.**(a). The relevant conductivity and relative permittivity data of the core, sheath and insulating layers are as follows: $\rho_c = 3.547 \times 10^{-8}\Omega\text{m}$, $\rho_s = 2.676 \times 10^{-8}\Omega\text{m}$, $\epsilon_{i1} = 2.89$, $\epsilon_{i2} = 2.3$. The cables are buried at a depth of 1.3 m with a separation of 0.4 m between them.

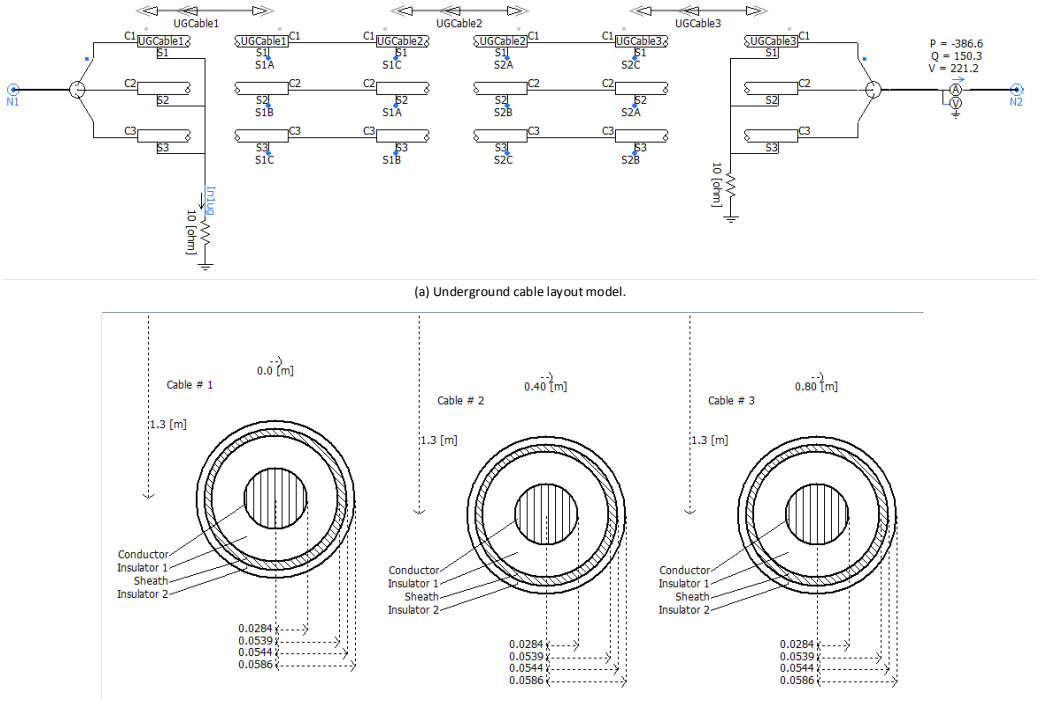

Fig. 6. Underground cable model.

Such a cable has unbalanced mutual coupling between the phases A and B, and A and C. Such an unbalance creates coupling between the sequence impedances. Hence it was decided to use trefoil layout of the cables in the PSCAD simulation and RSCAD implementation.

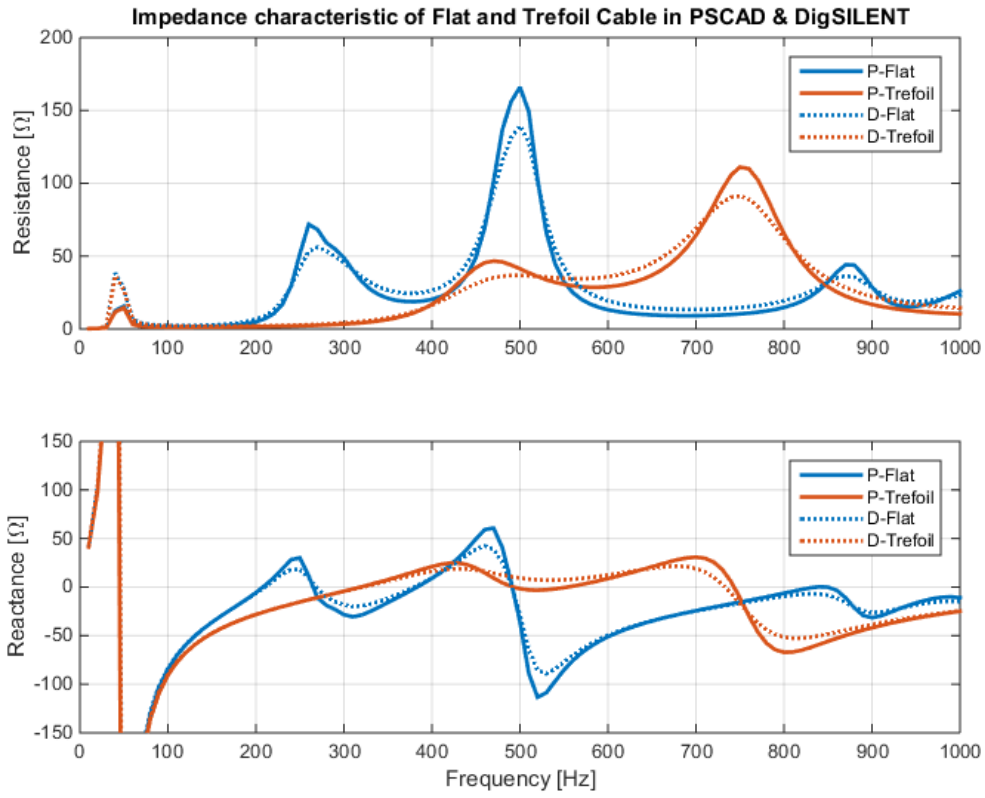

Fig. 7. Comparison of underground cable (in trefoil and in flat formation) impedance characteristics in DigSILENT and PSCAD.

1.1.2.3.2 Submarine Cable

The 24.5 km submarine cable is modelled as three conductor cores in trefoil formation. Only two conducting layers, viz. the core and the inner sheath have been included in the model so as to maintain the similarity of the models in DigSILENT and PSCAD models.

1.1.3 Harmonics compensation strategies

This section describes theoretical solutions identified on the basis of mathematical analysis and validated by PLECS simulation for harmonic compensation for the wind power plant (WPP) model. We use a simplified three-impedance model of the grid and WPP and study the harmonic compensation effectiveness at bus T1, when the STATCOM with active power filter (APF) is connected at bus T2. In all subsequent figures Z_1 is the equivalent grid impedance, Z_2 is the equivalent wind far m impedance, Z_T is the super-transformer impedance, and Z_{APF} is the virtual impedance created by the active power filter. The voltages at busses T1 and T2 are denoted by V_1 and V_2, and V_h is the harmonic source in the grid.

1.1.3.1 Compensation at T2 with voltage feedback from T1

This section describes a harmonic voltage controller based on the voltage feedback from bus T1. The WPP model in Fig. 8 shows the APF as a controlled current source that produces the current I_F as a function of the T1 voltage. Voltages V_1 and V_2 at busses T1 and T2, are given by (1).

$$V_1 = V_h \frac{Z_2+Z_T}{Z_1+Z_2+Z_T} - \frac{Z_1 Z_2}{Z_1+Z_2+Z_T} I_F \qquad V_2 = V_h \frac{Z_2}{Z_1+Z_2+Z_T} - \frac{(Z_1+Z_T)Z_2}{Z_1+Z_2+Z_T} I_F \qquad (1)$$

In the most general case the APF current is controlled by the T1 voltage by means of a virtual impedance Z_{APF}, as $I_F = KV_1/Z_{APF}$. Assuming the virtual impedance equal to Z_2, $Z_{APF} = Z_2$, the voltage at bus T1 is (2) and the filter current is $I_F = KV_1/Z_2$.

$$V_1 = V_h \frac{Z_2+Z_T}{(1+K)Z_1+(Z_2+Z_T)} \text{ or, } A_1 = \frac{V_1}{V_h} = \frac{Z_2+Z_T}{(1+K)Z_1+(Z_2+Z_T)} \qquad (2)$$

The static characteristic of the amplification ratio A_1 in (2) is shown in Fig. 9. It clearly shows, that the amplification ratio is unity for $k = -1$.

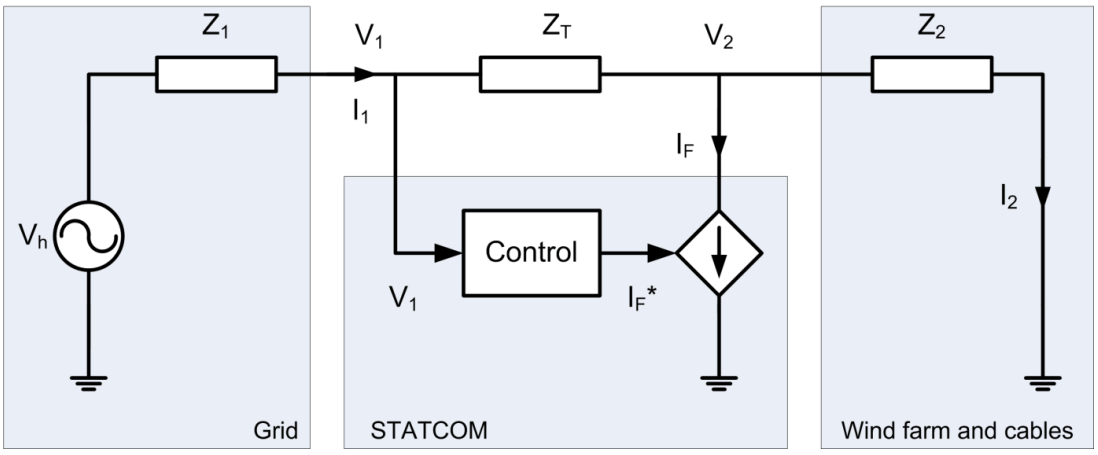

Fig. 8. Simplified wind farm model with compensation at T2 based on T1 voltage feedback.

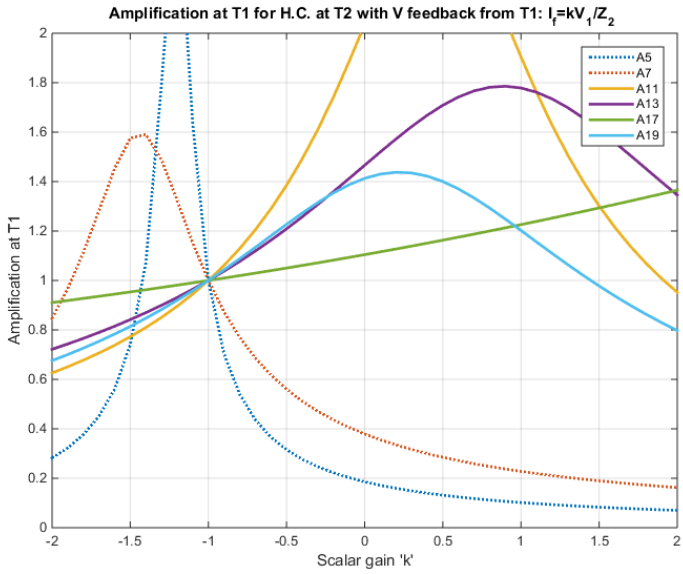

Fig. 9. Amplification at T1 due to the harmonic compensation at T2 using $I_f = \frac{kV_1}{Z_2}$

The goal is to keep the voltage magnitude at T1 equal to the grid voltage magnitude, i.e. $|V_1| = |V_h|$. This condition is satisfied by two values for gain *K*.

$$K_1 = -1 \qquad K_2 = -\frac{R_1^2+X_1^2+2R_1R_2+2R_1R_T+2X_1X_2+2X_1X_T}{R_1^2+X_1^2} \tag{3}$$

Solution K_1 is constant and always exists, while solution K_2 depends on all impedances and it is impractical for implementation as a controller with constant gain. However, it can be implemented by a closed loop feedback controller. Solution K_2 is positive for all cases when grid harmonics are amplified at T1 (h = 11, 13, 17, 19) and it is negative for other harmonic orders (h = 5, 7). Voltage V_1 can be reduced to any small value if K is large enough.

Similar solutions have been found for resistive feedback, $Z_{APF} = R_2$, and inductive feedback, $Z_{APF} = X_2$. In these cases all solutions depend on all impedance present in the system. The most advantageous for implementation is the gain $K_1 = -1$, which works for the complex virtual impedance case.

1.1.3.1.1 Dynamic analysis and Controller Design

For our case study, the grid and the WPP impedances are capacitive for harmonic orders *k* = 5 and 7. The voltage controller transfer function that implements the complex feedback, $I_F = KV_1/Z_2$ is (4)

$$H_{APF} = \frac{I_F^*}{V_1} = K\frac{C_2 s}{R_2C_2 s+1} \tag{4}$$

For harmonic orders *k* = 11 and above the WPP impedance is inductive, and the controller transfer function is (5).

$$H_{APF} = \frac{I_F^*}{V_1} = K\frac{1}{L_2 s+R_2} \tag{5}$$

The sign of gain *K* is of major importance for the controller stability: a positive gain creates a negative feedback loop, while a negative gain creates a positive feedback. Although the positive feedback can be stable under some circumstances (when the loop gain is less than unity), the negative feedback is always preferred. Thus, the simple solution K_1 = –1 in (6)

involves positive feedback and the stability of this solution must be carefully verified at implementation.

The reactive compensation, $Z_{APF} = X_2$, works with low filter currents at positive gains (negative feedback) and it is advantageous for implementation. The voltage controller that realizes $I_F = KV_1/X_2$ is a pure derivative transfer function as in (6), for harmonics *k* = 5 and 7. For a causal implementation this is combined with a low pass filter with a small time constant *T*.

$$H_{APF} = \frac{I_F^*}{V_1} = KC_2 s \cong K\frac{C_2 s}{Ts+1} \tag{6}$$

For harmonic orders *k* = 11 and above we use either a pure integrator, or a low pass filter (LPF) with a large time constant, *T*, as in (7). The LPF solution is practical for implementation.

$$H_{APF} = K\frac{1}{L_2 s} \cong K\frac{1}{Ts+1} \tag{7}$$

The resistive compensation, $I_F = KV_1/R_2$, can be realized with a real proportional gain.

In order to reduce the harmonics at values lower than the background levels the gain *K* has been adjusted using an integral controller with slow dynamic response (large time constant). Fig. 10 shows the block diagram of the complete controller used to reduce the harmonic voltage magnitude to a set value denoted by V_1^*. The block diagram shows the main controller H_{APF}, and the harmonic filter implemented in *dq* reference frame. This scheme has been implemented for each harmonic order.

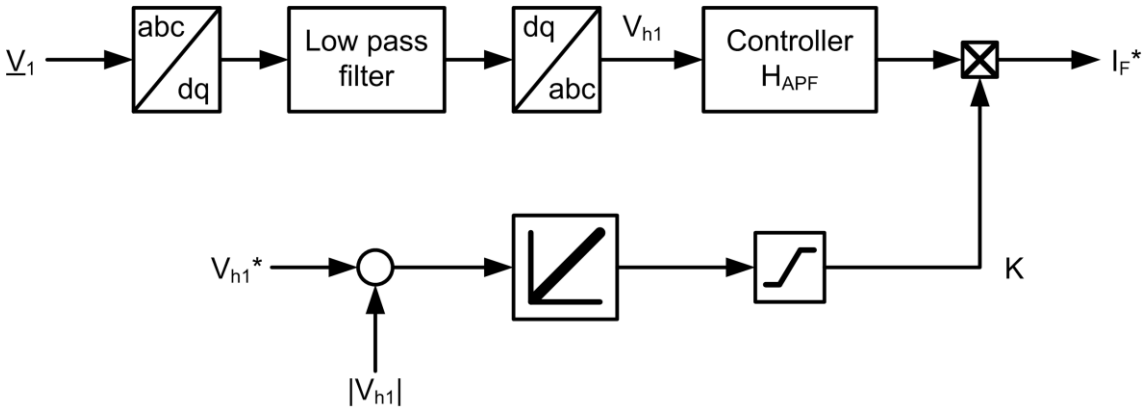

Fig. 10. Control block diagram for harmonic compensation at T2 based on T1 voltage feedback.

Complex compensation is stable for any positive gain *K*. Resistive compensation is unstable for harmonics *k* = 17 and 19 and approaches the instability limit for harmonics *k* = 11 and 13. Reactive compensation is stable for any positive gain *K*. The controller recommended for implementation is either the complex feedback (4) and (5) or the reactive feedback (6) and (7), both with positive gains (negative feedback). Apart from the different time constants, the two controllers are very similar. With negative gains (positive feedback) the system is stable for a narrow range, $K_{min} < K < 0$. The gain $K_1 = -1$, is stable for all harmonic orders and it can be used for implementation.

This analysis reveals the following aspects that characterize the T1 feedback control:

- The controller with feedback from T1 is able to reduce the harmonics to grid background levels.

- With large enough feedback gains the controller is able to reduce the harmonics to a value lower than the grid background levels.

- There is always one solution, $Z_{APF} = -Z_2$, that is independent of the grid impedance and that is constant as long as Z_2 stays constant.

- For reactive feedback the filter currents are lower.

- The filter current is lowest for the resistive feedback. This method is recommended for implementation.

1.1.3.2 Compensation at T2 with voltage feedback from T2

This section describes the harmonic compensation when the APF is connected at bus T2 and uses the voltage feedback from the same bus. The WPP model in Fig. 11 shows the APF as a current source that creates a virtual impedance Z_{APF}. The voltages V_1 and V_2 at busses T1 and T2, are (8).

$$V_1 = V_h \frac{Z_2 Z_{APF} + Z_T Z_2 + Z_T Z_{APF}}{Z_1 Z_2 + Z_1 Z_{APF} + Z_2 Z_{APF} + Z_T Z_2 + Z_T Z_{APF}} \qquad V_2 = V_h \frac{Z_2 Z_{APF}}{Z_1 Z_2 + Z_1 Z_{APF} + Z_2 Z_{APF} + Z_T Z_2 + Z_T Z_{APF}} \quad (8)$$

The APF current is controlled by the T2 voltage by means of a virtual impedance Z_{APF}, as $I_F = KV_2/Z_{APF}$. Assuming the virtual impedance equal to Z_2, $Z_{APF} = Z_2$, the voltage at bus T1 is

$$V_1 = V_h \frac{Z_2 Z_T (K+1) + Z_2^2}{Z_1 Z_2 (K+1) + Z_2 Z_T (K+1) + Z_2^2} \quad (9)$$

The goal is to keep the voltage magnitude at T1 equal to the grid voltage magnitude, i.e. $|V_1| = |V_h|$. This condition is satisfied by two values for gain K.

$$K_1 = -1 \qquad K_2 = -\frac{R_1^2 + X_1^2 + 2R_1 R_T + 2X_1 X_T + 2R_1 R_2 + 2X_1 X_2}{R_1^2 + X_1^2 + 2R_1 R_T + 2X_1 X_T} \quad (10)$$

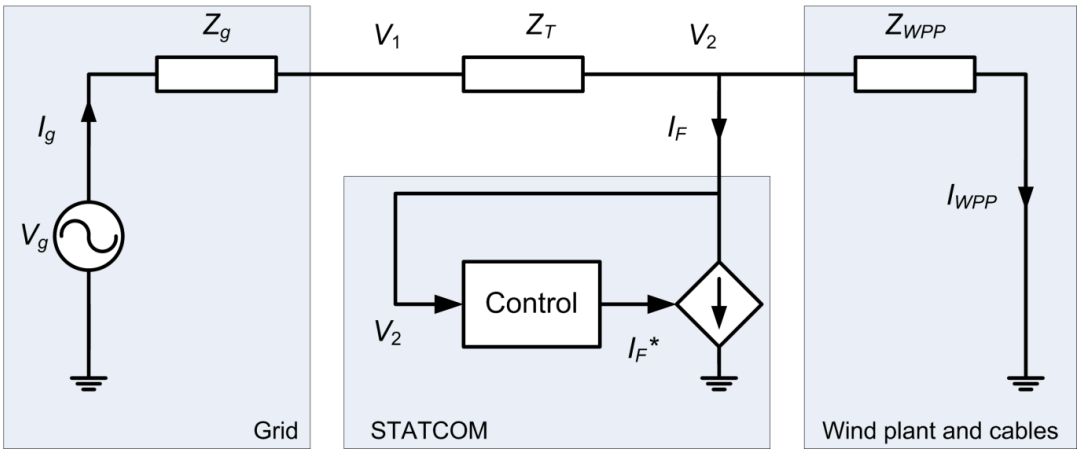

Fig. 11. Simplified model of the wind power farm and active filter for compensation at T2.

Solution K_1 is constant and always exists, while solution K_2 depends on all impedances and it is impractical for implementation. To implement this approach with a predetermined constant gain K, the APF current reference will be set to $I_F = KV_2/Z_2$.

A similar analysis have been carried out for resistive compensation, $Z_{APF} = R_2$, and for reactive compensation with $Z_{APF} = jX_2$. The solutions are quite similar in both cases. The conclusion is that the resistive and reactive compensation alone are unable to provide compensation

under all possible functional situations. Only the complex compensation is able to reduce the harmonics to background levels.

1.1.3.2.1 Dynamic analysis and Controller Design

The voltage controller transfer function that implements the complex feedback, $I_F = KV_2/Z_2$ is (11) for the case when Z_2 is capacitive and (12) for the case when Z_2 is inductive.

$$H_{APF} = \frac{I_F^*}{V_2} = K\frac{C_2 s}{R_2 C_2 s+1} \tag{11}$$

$$H_{APF} = \frac{I_F^*}{V_2} = K\frac{1}{L_2 s+R_2} \tag{12}$$

We analyzed the stability for this method and concluded the following. The sign of the gain *K* determines the feedback loop character: a positive gain creates a negative feedback, while a negative gain produces a positive feedback. Although the positive feedback can be stable under certain circumstances (when the loop gain is less than unity), the negative feedback is always preferred. Thus, the stability of the simple solution $K_1 = -1$ must be verified on implementation.

We analyzed the static performance of this compensation method based on voltage feedback from T2. The main conclusion is that it is difficult or impossible to achieve a significant reduction of harmonics below the background levels.

Different aspects that characterize the system can be concluded from this analysis:

- There are two solutions for the virtual impedance compensation that keep the harmonic voltages at their background levels;

- There is always one solution, $Z_{APF} = -Z_2$, that is independent of the grid impedance and that is constant as long as Z_2 stays constant. This solution is located on the boundary between stable and unstable operation.

- Resistive or reactive compensation at T1 is overall ineffective and fails to provide the harmonic reduction at T2 under all possible scenarios.

- Due to the nonlinear behavior, resonances, and instability risks, designing a feedback controller that provides attenuation for all situations seems to be a challenging task.

- Overall, it is difficult to achieve a significant reduction of harmonics below the background levels with virtual impedance at T2. This limitation is due to the large harmonic impedance of the super-transformer that provides a substantial separation between T1 and T2.

1.1.3.3 Equivalent impedance at T2 with compensation design at T1

In the WPP model shown in Fig. 12 the APF is connected at bus T2, and it creates a virtual impedance Z_{APF}. First we design a harmonic compensation at T1 in the form of Z_{T1}. Then, the equivalent APF impedance Z_{APF} connected at T2 that produces the same effect as Z_{T1} connected at T1 is calculated as

$$Z_{APF} = \frac{Z_{T1}Z_2^2}{(Z_2+Z_T)^2} - \frac{Z_T Z_2}{Z_2+Z_T} \tag{13}$$

If a resistive compensation is designed at T1, $Z_{T1} = R$, then the equivalent filter impedance is:

$$Z_{APF} = \frac{RZ_2^2}{(Z_2+Z_T)^2} - \frac{Z_T Z_2}{Z_2+Z_T} \qquad (14)$$

The virtual impedance Z_{APF} produces the same effect as Z_{T1} at T1. Its effect at T2 is different from that produced by Z_{T1} at T2.

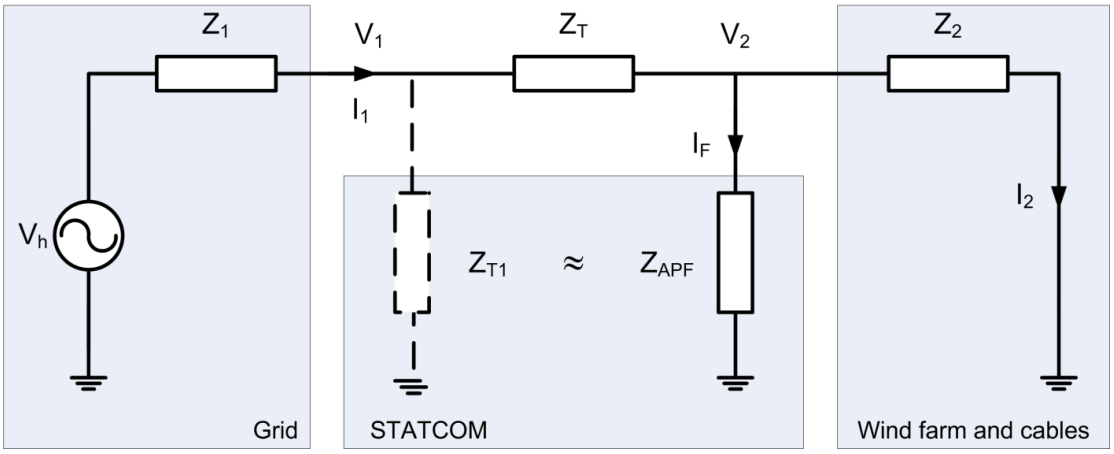

Fig. 12. Simplified model of the wind power farm and active filter for equivalent compensation at T2.

The implementation of complex or resistive compensation described by (13) and (14) is rather involved. In particular, for capacitive impedance Z_2, the transfer functions turn out being non-causal and cannot be implemented. On the other hand, similar functionality is provided by the current feedback controller described later. The current controller has a much simpler topology. For all these reasons, this equivalent controller has not been further investigated and a solution for implementation has not been developed.

1.1.3.4 Harmonic Compensation at T2 with Grid Current feedback

This section describes the harmonic compensation when grid current feedback is employed. The WPP model in Fig. 13 shows the APF current I_F controlled as a function of the grid current I_1, $I_F = KI_1$, where K is the gain of transfer function H_{APF} for each harmonic frequency. K can assume any real or complex value. The voltages at buses T1 and T2 are (15).

$$V_1 = V_h \frac{(1-K)Z_2+Z_T}{Z_1+Z_T+(1-K)Z_2} \qquad V_2 = V_h \frac{(1-K)Z_2}{Z_1+Z_T+(1-K)Z_2} \qquad (15)$$

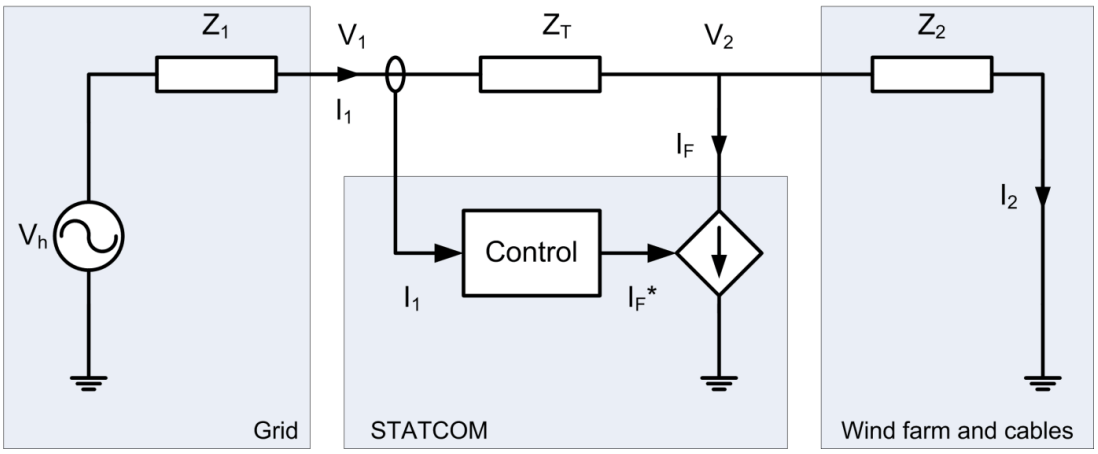

Fig. 13. Simplified wind farm model with compensation at T2 based on grid current feedback.

The goal is to have the voltage magnitude V_1 equal to grid voltage magnitude V_h. The solution of equation $|V_1| = |V_h|$ is the real gain K_1 in (16). For this case the compensation can be implemented using a simple proportional gain that multiplies the grid current, $I_F = K_1 I_1$.

$$K_1 = \frac{R_1^2+X_1^2+2R_1R_2+2R_1R_T+2X_1X_2+2X_1X_T}{2R_1R_2+2X_1X_2} \quad (16)$$

By analyzing the static performance of this scheme we found that the compensation with real gain *K* (i.e. a proportional feedback controller) is able to reduce the harmonics to the background levels, but it has difficulties to reduce them to values below the background levels.

The voltage at T1 can be reduced below the background levels, all the way down to zero by using a dynamic controller. The solution for equation $V_1 = 0$ is (17). This solution does not depend on the grid impedance Z_1. The voltage at bus T2 can also be reduced to zero with $K = 1$.

$$K_0 = \frac{Z_2+Z_T}{Z_2} \quad (17)$$

The compensation with complex feedback can be implemented as in (18).

$$I_F = K\frac{Z_2+Z_T}{Z_2} I_1 \quad (18)$$

1.1.3.4.1 Dynamic analysis and Controller Design

The controller transfer function that provides proportional (P) feedback is (13).

$$H_{APF} = \frac{I_F^*}{I_1} = K \quad (19)$$

The gain *K* must be negative in order for the control system to work with stable negative feedback.

The controller transfer function that provides complex feedback can be implemented as a proportional-integral (PI) controller (20).

$$H_{APF} = \frac{I_F^*}{I_1} = K(R - \frac{\omega}{s}X) \quad (20)$$

where *R* and *X* are the resistance and reactance of the equivalent impedance $Z = (Z_2 + Z_T)/Z_2$.

In order to reduce the harmonics at values lower than the background levels the gain *K* has been adjusted using an integral controller with slow dynamic response (large time constant). Fig. 14 shows the block diagram of the complete controller used to reduce the harmonic voltage magnitude to a set value denoted by V_1^*. The block diagram shows the main controller H_{APF}, and the harmonic filter implemented in *dq* reference frame. This scheme must be implemented for each harmonic order.

To verified the stability for this simplified model using the root locus of the open-loop transfer function $H_0 = H_1 H_{APF}$ for each harmonic order. The P controller has the advantage to preserve the order of (11) or (12), i.e. the closed loop control system is of second order. This controller is stable for any negative gain *K*. The PI controller increases the system order by adding a zero pole.

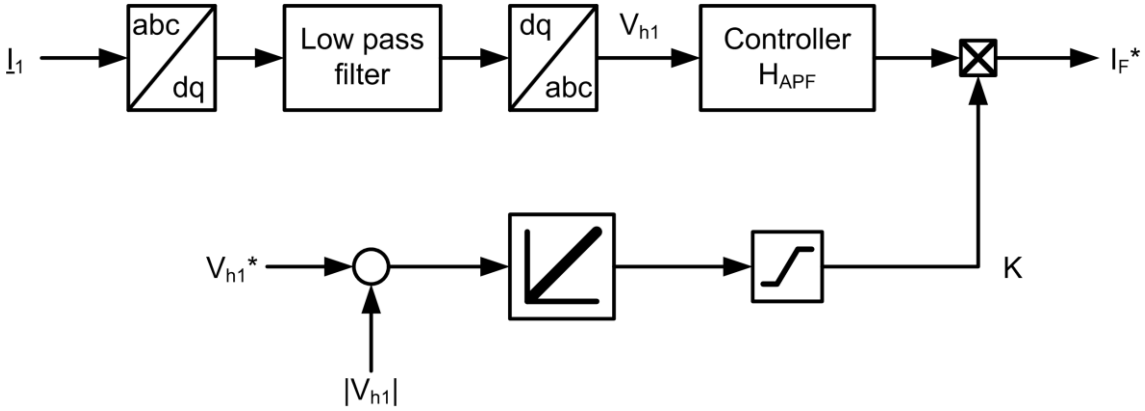

Fig. 14. Control block diagram for harmonic compensation at T2 based on Grid current feedback.

We conclude that both controllers are adequate for implementation. The P controller is very simple and provides harmonic attenuation to background levels. The PI controller adds a pole and increases the system complexity, but it is able to reduce the harmonics to any value below background levels, all the way to zero.

1.1.3.5 Harmonic Compensation at T2 with Wind Farm Current Feedback

Fig 7 shows the simplified WPP model when the filter current is controlled as a function of the wind farm current I_2, using the feedback controller with transfer function H_{APF}. In this case the filter current is (21) and the T1 voltage is (22).

$$I_F = KI_2 = K\frac{V_2}{Z_2} \tag{21}$$

$$V_1 = V_h \frac{Z_2+(1+K)Z_T}{(1+K)(Z_1+Z_T)+Z_2} \tag{22}$$

This case is the same compensation solution described in Chapter 2, as virtual impedance at T2. All solutions and all conclusions presented in Chapter 2 remain valid for this case. There are two solutions for harmonic compensation. The simplest one is $K = -1$, which is marginally stable, while the second one depends on Z_1. This case will not be further discussed.

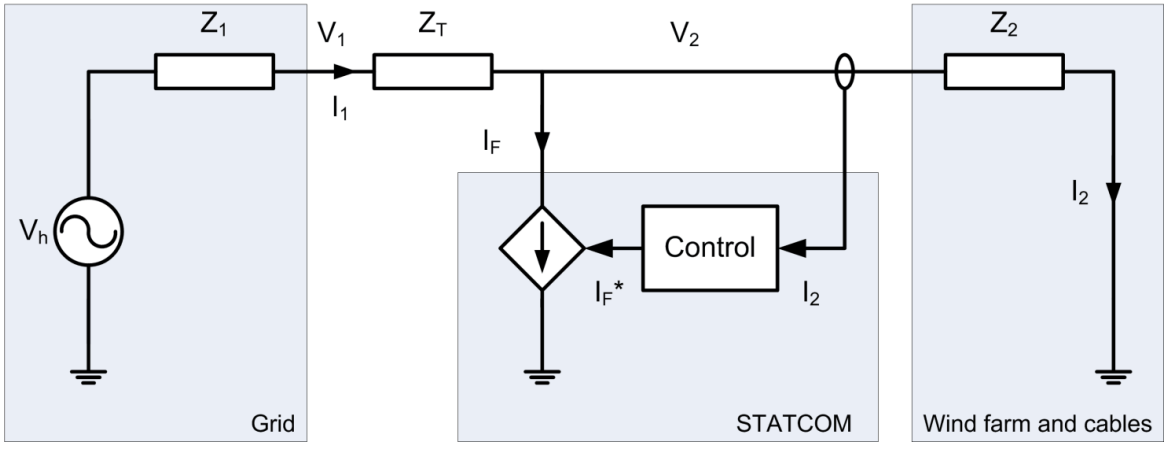

Fig. 7 Simplified wind farm model with compensation at T2 based on WPP current feedback.

This analysis reveals the following aspects that characterize the current feedback control:

- We identified two solutions based on grid current feedback which are able to reduce the voltage harmonics at bus T1.

- The first solution is a simple proportional controller that is able to reduce the harmonics to grid background levels. The closed-loop system with P control is stable for any negative gain.

- The second solution is a proportional integral controller that is able to reduce the harmonics to any value lower than the grid background levels. The closed-loop system with PI control is stable for any positive gain.

- The compensation based on grid current feedback is simple and easy to implement. In conclusion, the grid current control is recommended for implementation.

1.1.3.6 Conclusion

We have described five distinct methods for harmonic compensation for the wind power plant simplified model. All methods work with remote compensation – harmonic reduction at T1 with current injection at T2.

For each method we provide a steady-state analysis that identifies one or more controller topologies which are able to reduce the harmonics to the grid background levels or to lower values. A stability analysis that identifies a range of gains for which the closed-loop control system is stable is also provided for each method. Table I summarizes the most important properties of the remote compensation methods proposed here.

Table I Main properties of harmonic compensation methods

	T2 voltage feedback (§1.5.3.2)	Equivalent impedance at T2 (§1.5.3.3)	T1 voltage feedback (§1.5.3.1)	Grid current feedback (§1.5.3.4)
Remote compensation at T1	Yes	Yes	Yes	Yes
Reduces harmonics to grid background levels	Yes	Yes	Yes	Yes
Reduces harmonics to zero	No	Yes	Yes	Yes
Theoretical stability	Yes	n/a	Yes	Yes
Stable in RSCAD simulation	n/a	n/a	Yes	Yes
Number of sub-methods	Real and complex	Complex	Real and complex	Real and complex
Control complexity	simple	complex	simple	simple
Sensors required	voltage	voltage	voltage	current
Sensor bandwidth	1 kHz	1 kHz	1 kHz	1 kHz
Recommended	No	No	Yes	Yes

It is concluded that the most promising methods are the compensation based on T1 voltage feedback and compensation based on grid current feedback. Therefore, these schemes have been selected for PSCAD implementation and validation.

1.1.4 PSCAD simulation results (Resistive, kV1/Z2 for ID24)

The method described in T1 voltage feedback (§1.5.3.1) was implemented in PSCAD for the two sub-cases:

1. Constant gain such that, the compensating filter current is given by, $I_f = -k\frac{V_1}{Z_2}$. the harmonic voltage amplification at T1 should be unity as per (2). Thus the harmonic voltages at T1 should be limited to the background levels.

2. Adaptive gain, where, the compensating filter current is given by, $I_f = -k\frac{V_1}{Z_2}$, and the gain k is obtained by integrating the measure of excess harmonic voltage above the specified limiting levels as shown in Fig. 10.

For this purpose, the effective WPP impedance (Z_2) at a particular harmonic order has been converted into equivalent R-L or R-C elements and relevant time constant for the transfer functions as shown in Table II. It considers the collector grid cables and the underground cables in trefoil formation.

Table II Conversion of the WPP harmonic impedance data to equivalent R, and L or C components.

Freq(Hz)	R(Ohm)	X(Ohm)	L(H)	C(F)	tau(sec)
50	54.15	54.83	1.75E-01	-5.81E-05	-3.14E-03
250	6.11	-50.93	-3.24E-02	1.25E-05	7.64E-05
350	4.94	-28.55	-1.30E-02	1.59E-05	7.87E-05
550	6.44	-10.70	-3.10E-03	2.70E-05	1.74E-04
650	8.27	-3.97	-9.72E-04	6.17E-05	5.10E-04
850	9.25	-0.43	-8.08E-05	4.34E-04	4.01E-03
950	10.01	2.54	4.25E-04	-6.60E-05	-6.60E-04

These impedances are emulated to generate the corresponding harmonic current references from the corresponding harmonic sequence voltages as shown in the block diagram in Fig. 14**Error! Reference source not found.**. The block diagram also shows the extraction of the sequence components using the Park's transformation, first order filters and the inverse park's transformation. Finally the extracted voltage is multiplied with the WPP admittance transfer function to obtain the reference currents for the filter.

1.1.4.1 Compensation with constant gain k=1.

The method has been successfully applied in all the 24 grid impedance cases. In every case, the harmonic voltages tend to approach the background levels is indicated in the first row. While the 13th harmonic is amplified in all the cases, the 19th harmonic gets amplified only in the case ID 24. In some cases, like ID=3, 4, 11, 13 and 14, the 13th harmonic voltage is amplified from 0.5% in the background to 1.19%, 1.16%, 1.16, 1.14 and 1.18% respectively. These results are summarized in Table III , which shows the base case and compensated case values of the 5th, 7th, 11th, 13th, 17th and the 19th harmonic components. In all these case,

the 13th harmonic voltage in the compensated case is limited within 0.544%. The 5th, 7th, and 11th harmonic cases are well attenuated in all these cases. They are included in this simulation and the report just for the sake of theoretical justification that the voltages tend to move to the background levels. These cases do not have practical significance, as the attenuated harmonic levels are preferable.

Table III Simulation of the 24 cases and the effect of harmonic compensation, $I_f = -\frac{V_1}{Z_2}$

Harmonics	V5N	V7P	V11N	V13P	V17N	V19P
Back-	0.50%	0.34%	0.44%	0.49%	0.10%	0.42%
ID=3, Base	0.402%	0.166%	0.156%	1.193%	0.096%	0.382%
ID=3,	0.472%	0.336%	0.391%	0.544%	0.100%	0.417%
ID=4, Base	0.408%	0.148%	0.173%	1.162%	0.096%	0.382%
ID=4,	0.472%	0.328%	0.398%	0.543%	0.100%	0.417%
ID=11,	0.402%	0.146%	0.171%	1.157%	0.096%	0.383%
ID=11,	0.470%	0.329%	0.413%	0.542%	0.100%	0.417%
ID=13,	0.407%	0.151%	0.166%	1.141%	0.096%	0.382%
ID=13,	0.472%	0.327%	0.400%	0.542%	0.100%	0.417%
ID=14,	0.408%	0.148%	0.176%	1.182%	0.096%	0.382%
ID=14,	0.472%	0.328%	0.404%	0.544%	0.100%	0.417%

It must be however, noted that these are the positive or negative sequence voltages as indicated by the suffix 'N' or 'P' after the harmonic number – 5, 7, 11, 13, 17, and 19.

1.1.4.2 Compensation with adaptive gain k, obtained by the integration of harmonic level above the limits

The method has been successfully applied for the case ID24. The time domain simulation results are shown in Fig. 15**Error! Reference source not found.**. In the beginning of the simulation, the harmonic compensator gain is 0, i.e. it is disabled. It is activated at the time instant 10s. Since the 11th, 13th and the 19th harmonics are above limits, the gain k starts to increase for the harmonic orders as the error is positive. For the other three harmonics, the error is negative and hence the gains k remain unchanged. After around 60 seconds, the harmonic levels settle close to the desired limit levels. The 5th, 7th, and 17th order harmonics remain unchanged as they are under the harmonic limits.

Table IV. Harmonic voltage levels and their limits, at T1 in the base and compensated cases.

Harmonics	Background	Limits	Base	Compensated
	0.50%	0.40%	0.30%	0.30%
7	0.34%	0.30%	0.25%	0.25%
11	0.44%	0.30%	0.54%	0.30%
13	0.49%	0.20%	0.56%	0.20%
17	0.10%	0.20%	0.10%	0.10%
19	0.42%	0.150%	0.47%	0.15%

The background harmonic voltage levels in the grid and their limits along with the levels in the base case are compared with the levels attained after compensation in Table IV. Fig. 16compares the harmonic voltage levels in the base case and after compensation at the HV buses T1, T2, T3, and T4. The compensation leads to a good attenuation of the 11th, 13th and

19th harmonics at bus T1. However, there is an amplification of the harmonic voltage levels at other buses, T2, T3 and T4 which are within the WPP. The harmonic voltages at T1 are brought down to the specified limit levels. However, as shown in Fig. 16, the harmonic voltage levels are very much amplified at the other buses, viz. T2, T3 and T4 within the WPP. The 13th and 19th order harmonic voltages are amplified to 2.4% while the 11th order is amplified to 1.5%.

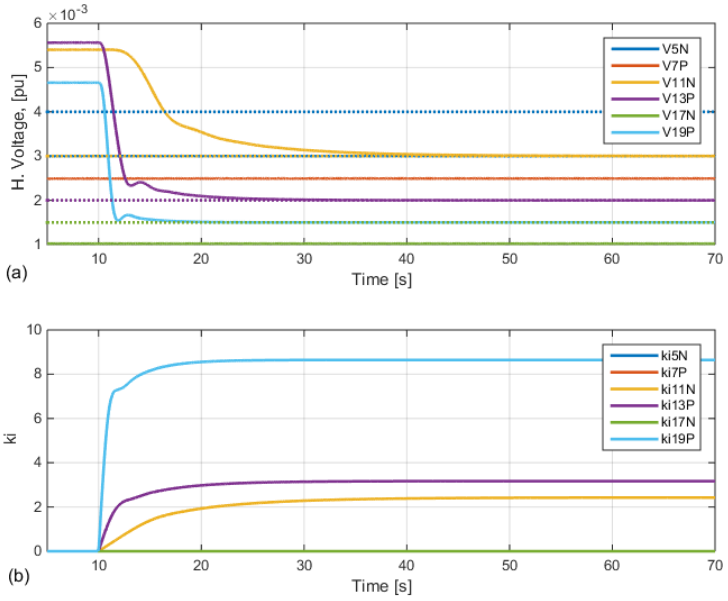

Fig. 15. Harmonic compensation at T2 using voltage at T1 (a) Variation of the harmonic voltage levels. (b) Variation of the integral gain constants.

Table V. Harmonic voltage levels at T2, T3 and T4 in the base case and after compensation.

Bus	T2		T3		T4	
Harmonic	Base	Comp.	Base	Comp.	Base	Comp.
11	0.17%	1.54%	0.07%	0.65%	0.14%	1.24%
13	0.18%	2.42%	0.06%	0.82%	0.13%	1.76%
19	0.05%	2.40%	0.04%	1.58%	0.05%	2.16%

Table VI. Amplification of harmonic current flows and the STATCOM harmonic currents (1pu is 649.5 A rms at T1, and 1141.6 A at T2, T3, T4 and STATCOM).

Bus	T1		T2		T3		T4		STATCOM
Harmonic	Base	Comp.	Base	Comp.	Base	Comp.	Base	Comp.	Comp.
11	0.61%	1.85%	0.61%	5.42%	0.66%	5.86%	0.10%	0.87%	6.2%
13	0.58%	2.35%	0.58%	7.69%	0.69%	9.04%	0.09%	1.19%	7.7%
19	0.35%	1.63%	0.35%	15.19%	0.24%	10.33%	0.01%	0.44%	14.50%

The compensation results in an increased level of harmonic current flows in the grid as well as in the WPP network as shown in Fig. 17. The values are tabulated in Table VI. Maximum harmonic currents are observed at T2, where it is 15% of the nominal current level (considering a base of 450 MVA, and 227 kV) at the 19th harmonic, and 8% of the nominal for the 13th

harmonic. The compensating harmonic currents in the STATCOM currents are 6.2%, 7.7% and 14.5% respectively for the 11th, 13th and the 19th order harmonics as shown in Table VI.

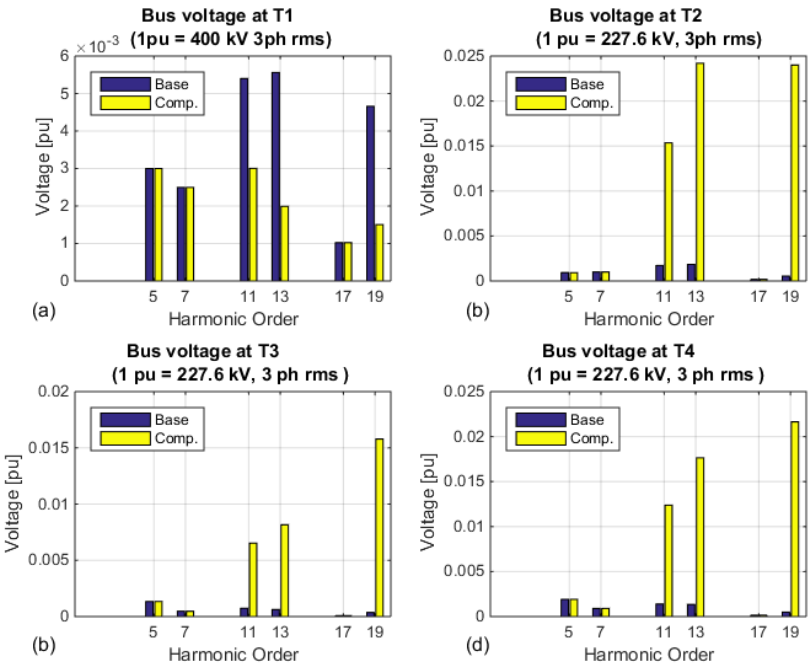

Fig. 16. Harmonic voltage levels at T1, T2, T3 and T4.

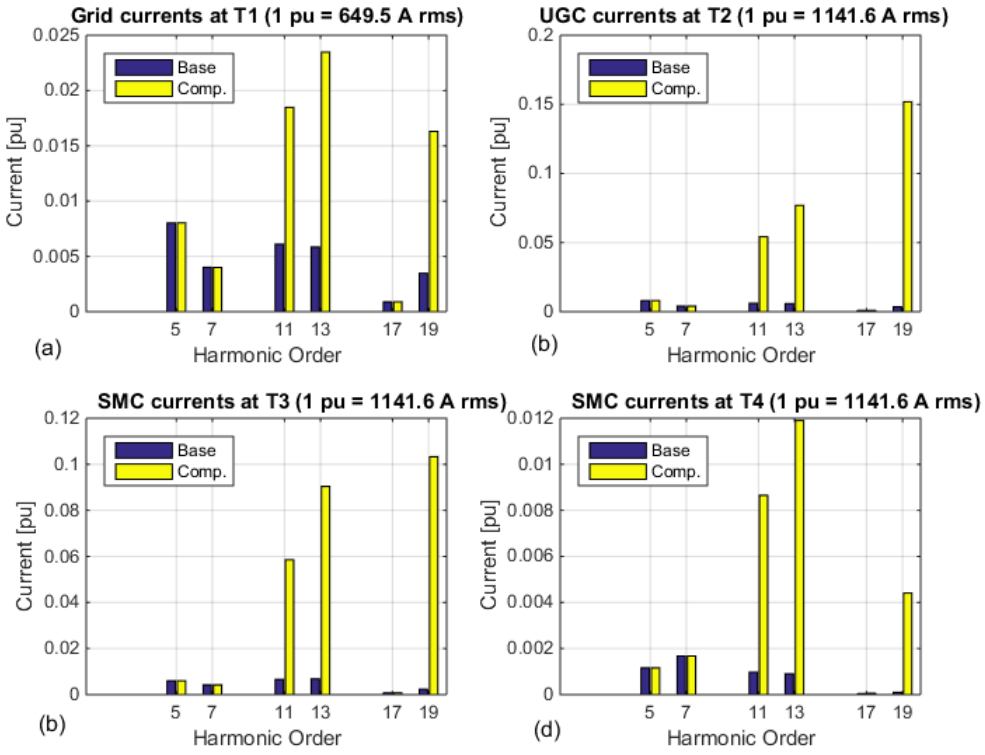

Fig. 17. Harmonic current flow. (a) Grid at t1. (b) UG cable at T2. (c) SM cable at T3. (d) SM cable at T4.

The robustness of the control method against variation in the WPP layout configuration was studied by varying the amount of HV cables in the export cable system. Just for the sake of variation, the underground cable and the submarine cables were duplicated. The reactors for the reactive power compensation were not changed, so there is excessive var generation in the system. The following events were studied:

1. At time 10s, the controllers are enabled in the base case.

2. At time 50s, second submarine cable is switched in.

3. At the instant 90s, the second underground cable is switched in.

4. At the instant 130s, the second SM cable is switched off.

The variation in the controller gain 'k' and the corresponding harmonic voltages under the changing grid conditions are shown in Fig. 18**Error! Reference source not found.**. Each cable switching event creates a deviation in the harmonic voltage level at bus T1. As the desired harmonic limits are exceeded, the integral gain changes and the harmonic voltages are brought down to the limits. In the simulation, the case with a single UG cable and 2 SM cable seems to have poor damping as there are large oscillations in the beginning and it takes longer time to settle down. This could be due to the high integral gains (2500, 400 and 125 for the 19^{th}, 13^{th} and the 11^{th} harmonic orders respectively) used in the controller gain constants. It was necessary to use a fast integrator so as to minimize the simulation runtime to 200s. In real time simulation and practical installations, such a fast integrator would not be necessary.

Nevertheless, the controller is stable in all the cases studied so far.

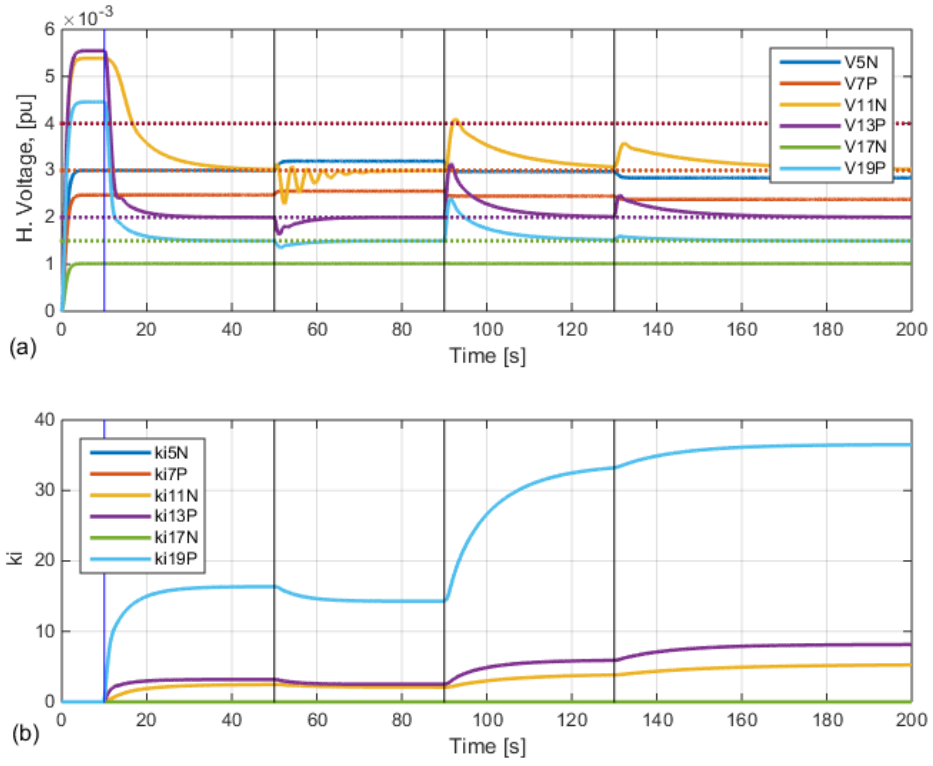

Fig. 18. Harmonic voltage levels and corresponding gain constant 'k' during different combinations of the HV export cables.(i) Up to 50 s, 1 UG cable+ 1 SM cable. (ii) From 50 s to 90 s, 1 UG cable and 2 SM cable. (iii) From 90 s to 130 s, 2 UG cable and 2 SM cable. (iv)From 130 s to 200 s, 2 UG cable and 1 SM cable.

1.1.4.3 Conclusion

A harmonic current compensator has been designed at bus T2, using the voltage measurements from the bus T1. It is able to hold the harmonic levels close to the background levels using gain k=-1 (reported in the previous month). The gain k can be adjusted by integrating the error between the observed harmonic levels and the desired harmonic voltage limits for each harmonic order. The harmonic voltages were successfully controlled to the desired limit levels, which were lower than the background harmonic levels for the 11th, 13th and the 19th harmonic orders. However, this led to excessive increase in the harmonic voltage levels at the bus T2, T3 and T4 in the WPP network. The 13th and 19th order harmonic voltages at T2 were amplified to 2.4% of the nominal voltage (i.e. 227 kV). The STATCOM harmonic current was 6.2%, 7.7% and 14.5% respectively for the 11th, 13th and the 19th order harmonics.

1.1.5 Experimental validation in RTDS

Since it takes a long time to simulate different cases with different control algorithms in PSCAD, it was decided to model the the plant in RSCAD and test the different control methods.

1.1.5.1 Schematic

The plant schematic for simulation in RSCAD is shown in Fig. 19.

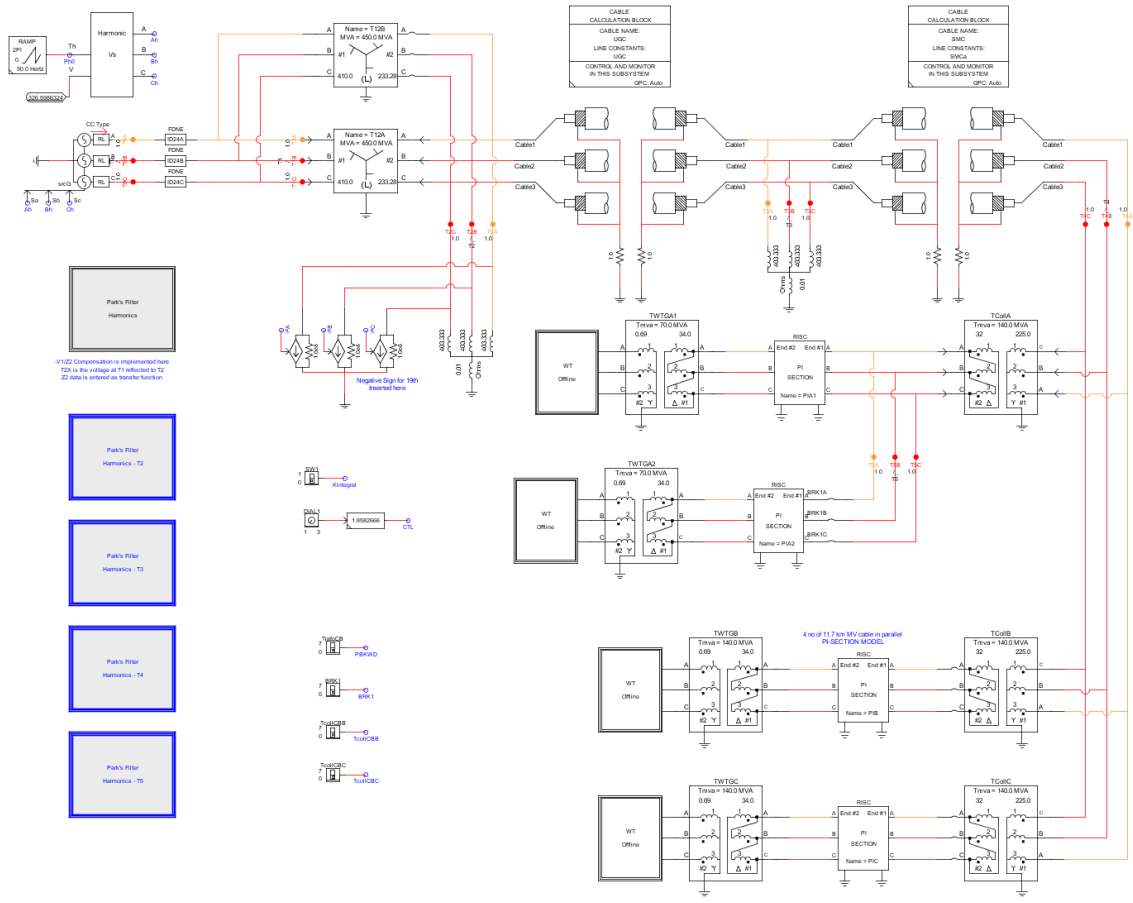

Fig. 19. Plant schematic in RSCAD

1.1.5.2 Simulation results with method using T1 voltage feedback (§1.5.3.1)

The harmnonic compensation using the voltage feedback method proposed in 1.5.3.1 has been implemented in the STATCOM controller in RSCAD. The base case harmonic voltages present in the base case and after compensation using constant value of the k in the voltage

feedback is shown in Fig. 20. As predicted, the harmonic voltages at the bus T1 is limited at the background levels. When an adaptive gain is used, the harmonic voltages at the bus T1 can be brought down to low levels as specified in the reference limits, even lower than the background levels as shown in Fig. 21. It also shows dynamics of the reduction of the harmonic voltages at T1 as the adaptive gain K is increasing in the time domain simulation. The compensating currents supplied by the STATCOM is shown in Fig. 22.

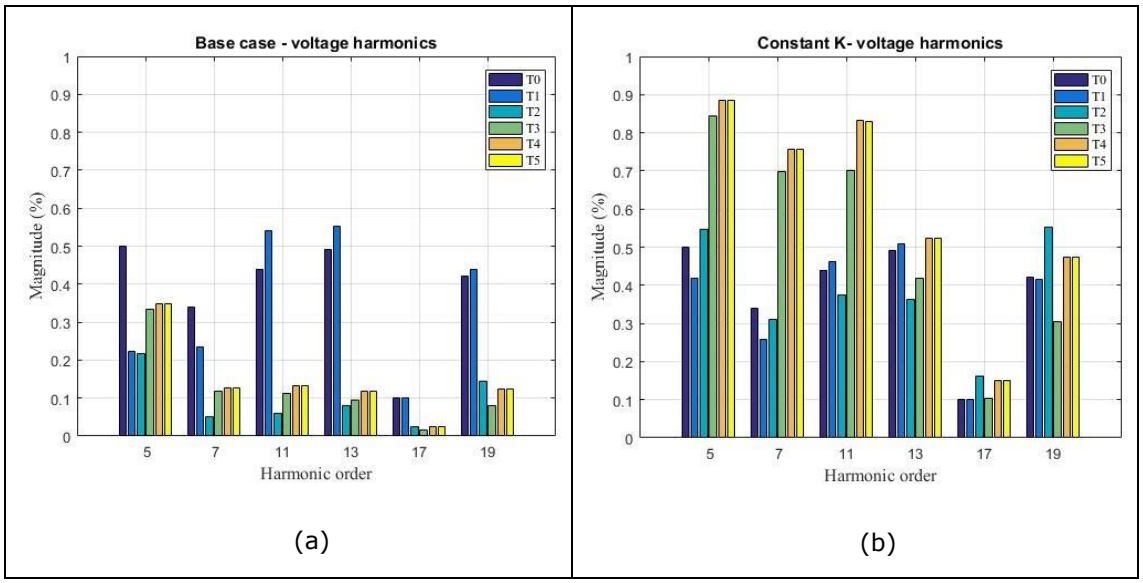

Fig. 20. (a) Without compensation: k=0. (b) Constant compensation: k=1

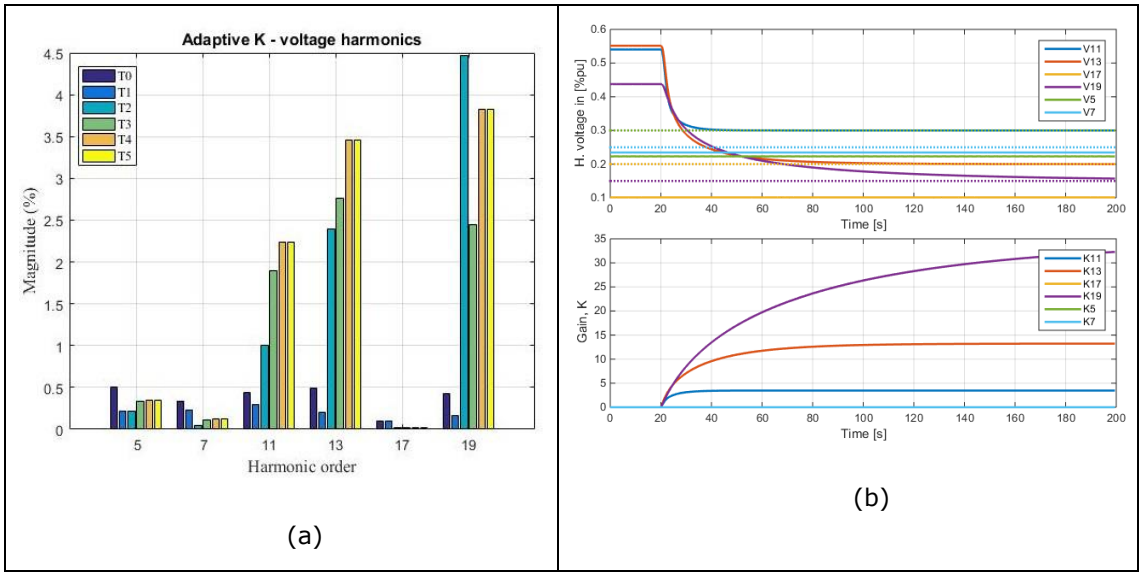

Fig. 21. (a) Adaptive compensation: k=~. (b)Compensation activation and corresponding gains

Table VII shows the numerical values of the harmonic voltages at all the high voltage terminals in the WPP when the constant gain (i.e. K=1) is applied in the voltage feedback to bring the harmonic voltages at the 400 kV bus to the background levels. These voltages can be brought down to even lower levels as Table VIII by applying an adaptive gain K as described before. However, this leads to a higher harmonic voltage levels at the busses inside the WPP, such as 4.8% of the 19th harmonic at voltage appears at T3, when the method is used to limit this harmonic voltage to 0.15% at T1. .

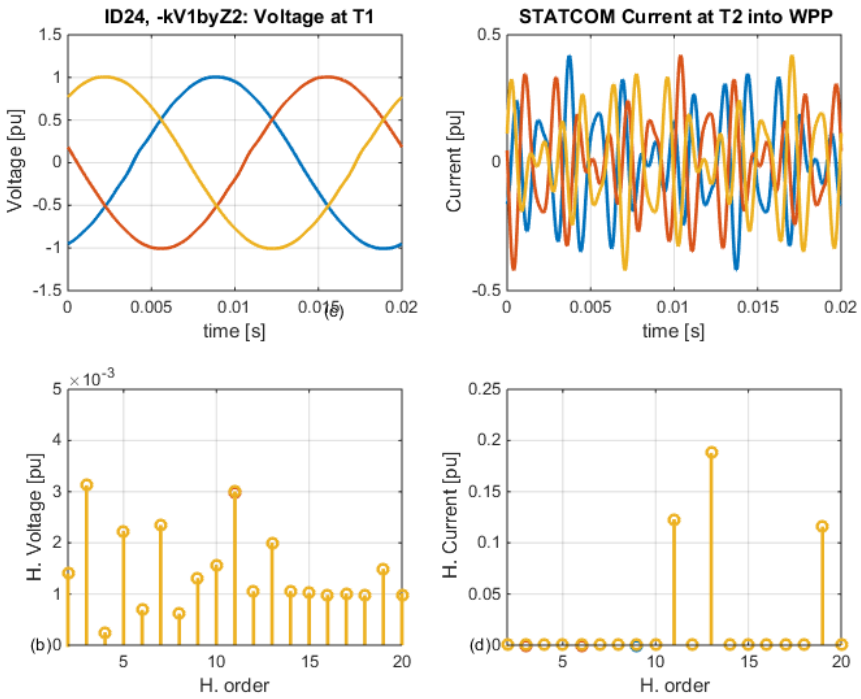

Fig. 22. Case ID=24 with voltage feedback from T1 and adaptive gain ($K_{11} = 3.5, K_{13} = 13, and\ K_{19} = 35$). (a)Voltage waveform at T1. (b) Voltage harmonics at T1 (in pu). (c) STATCOM currents waveform. (d) STACOM current harmonics.

Table VII. Voltage harmonics at T1 and STATCOM harmonics currents in Case ID=24 with complex feedback of voltage from T1, and constant feedback gain, K=1

Harmonic	5th	7th	11th	13th	17th	19th
Background	0.5	0.34	0.44	0.49	0.1	0.42
T1	0.22	0.23	0.44	0.49	0.10	0.42
T2	0.22	0.05	0.45	0.49	0.03	0.42
T3	0.33	0.12	0.85	0.57	0.02	0.23
T4	0.35	0.13	1.01	0.71	0.02	0.36
T5	0.35	0.13	1.01	0.71	0.02	0.36
Current, If	0.00	0.00	5.18	3.33	0.00	0.74

Table VIII. Voltage harmonics at T1 and STATCOM harmonics currents in Case ID=24 with complex feedback of voltage from T1, and adaptive feedback gain

Case ID 24	5	7	11	13	17	19
Background	**0.5**	**0.34**	**0.44**	**0.49**	**0.2**	**0.42**
Limit	**0.4**	**0.3**	**0.3**	**0.2**	**0.2**	**0.15**
T1	0.22	0.23	0.30	0.20	0.10	0.15
T2	0.22	0.05	1.01	2.39	0.03	4.80
T3	0.33	0.12	1.89	2.76	0.02	2.64
T4	0.35	0.13	2.24	3.45	0.02	4.12
T5	0.35	0.13	2.23	3.45	0.02	4.12
Current, If	0.00	0.00	12.30	18.79	0.00	11.60

1.1.5.3 Instability of adaptive harmonic compensation

This section illustrates the reason for instability of proposed method observed under particular cases in both PSCAD and RSCAD. Fig. 23 shows the amplification of harmonics at T1 resulting from compensation (STATCOM) at T2. The control law for the harmonic compensation depends upon the slope of the harmonic voltage curve vs. the gain k around the point 0 and −1. If the slop is negative, the compensation action amplifies the harmonic voltage magnitude and hence the control loop becomes unstable. It is stable if the slope is positive. For instance, for case 3 (grid impedance snapshot 3), the slopes on left side of -1 are positive for all harmonics except 13th, which means that the control is only stable for harmonic 13th. Therefore, only the 19th harmonic would create problem in case 3, as other harmonics are well attenuated in the base case itself. Hence their adaptive gains resulting from integral element remain unchanged at 0. The curves have been analyzed for all the cases with 24 different grid impedance scans. The slopes for some of the selected cases are summarized in Table IX. The slope is always negative for all harmonic 5th and 7th in all the cases. Same trend is observed for harmonics 17th and 19th, except for the case 24. In contrast, the slopes are consistently positive for harmonic 13th in all cases and different signs for harmonic 11th.

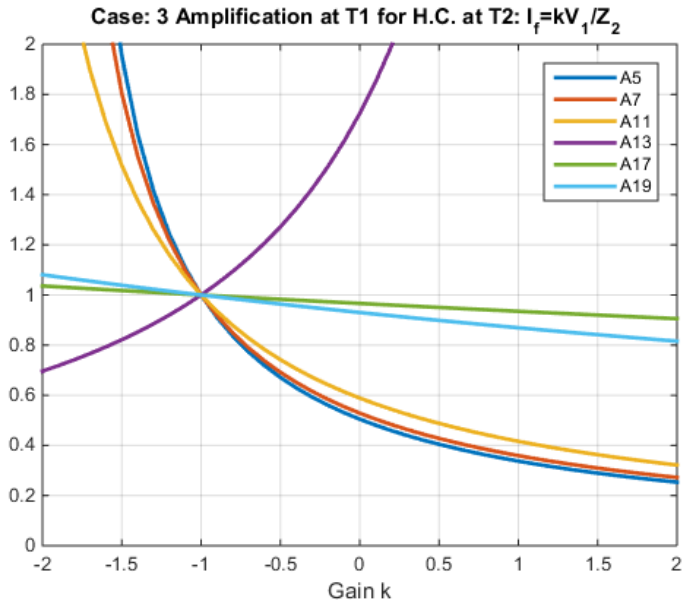

Fig. 23. Variation of the harmonic amplification ratio at T1 vs the adaptive gain 'k'.

Table IX Slope of harmonic voltage curve vs. the gain k on left side of -1.

Case ID	S5	S7	S11	S13	S17	S19
1	-1.09	-0.7	0.9	0.08	-0.02	-0.07
2	-1.06	-0.52	0.77	0.1	-0.02	-0.07
3	-1.09	-0.98	-0.74	0.41	-0.03	-0.08
4	-0.91	-1.2	-0.84	0.42	-0.03	-0.08
5	-0.85	-0.58	0.79	0.10	-0.02	-0.07
24	-6.49	-2.04	0.57	0.44	0.06	0.23

Case ID=1 is simulated with this modification. the harmonic voltage levels at t1 and corresponding compensating currents are shown in Fig. 24.

1.1.5.4 Simulation of Case ID24: T1 voltage feedback (§1.5.3.1) with real feedback

A variation of generating the compensating current references by providing real voltage feedback can be achieved by using $I_F = KV_1/R_2$. Like the previous case, this method, too, is able

to drive the harmonic voltages at t1 to the background levels as given in Table X and to much lower levels as shown in Table XI. The performance is quite sim8ilar in terms of the magnitude of the compensating current. Even the harmonic amplification at the busses within the WPP is similar. The biggest advantage of this method si it does not depend upon the WPP impendace.

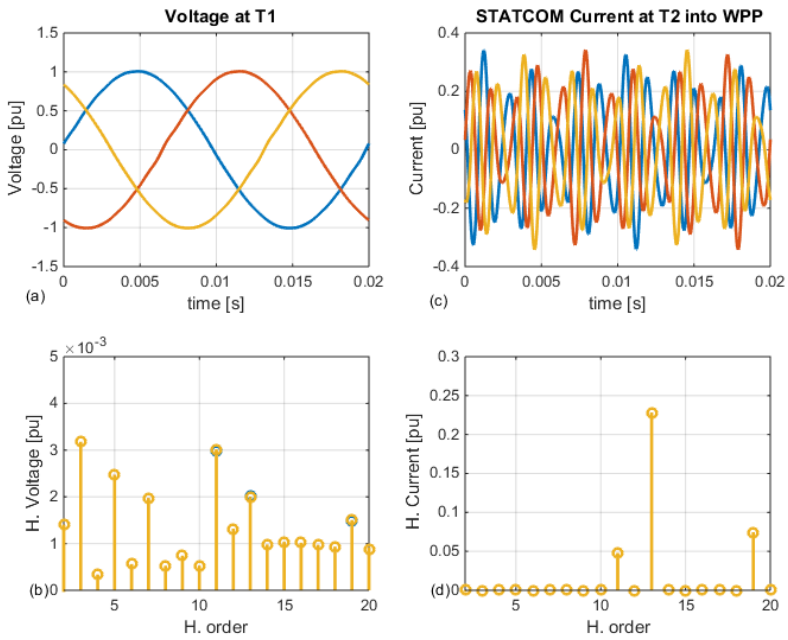

Fig. 24. Case ID=01 with voltage feedback from T1 and $K_{11} = 1.4, K_{13} = 16, \& K_{19} = -22$. (a)Voltage waveform at T1. (b) Voltage harmonics at T1 (in pu). (c) STATCOM currents waveform. (d) STACOM current harmonics.

Table X. Voltage harmonics at T1 and STATCOM harmonics currents in Case ID=24 with real feedback of voltage from T1 to drive the harmonics to background levels

Harmonic	5th	7th	11th	13th	17th	19th
Background	0.5	0.34	0.44	0.49	0.1	0.42
T1	0.22	0.23	0.44	0.49	0.10	0.42
T2	0.22	0.05	0.45	0.55	0.03	0.39
T3	0.33	0.12	0.85	0.64	0.02	0.21
T4	0.35	0.13	1.01	0.80	0.02	0.34
T5	0.35	0.13	1.01	0.80	0.02	0.34
Current, If	0.00	0.00	5.47	4.14	0.00	0.72

Table XI Voltage harmonics at T1 and STATCOM harmonics currents in Case ID=24 with real feedback of voltage from T1, and adaptive feedback gain

Harmonic	5	7	11	13	17	19
Background	**0.5**	**0.34**	**0.44**	**0.49**	**0.2**	**0.42**
Limit	**0.4**	**0.3**	**0.3**	**0.2**	**0.2**	**0.15**
T1	0.22	0.23	0.30	0.20	0.10	0.15
T2	0.22	0.05	1.03	2.57	0.03	4.80
T3	0.33	0.12	1.93	2.97	0.02	2.63
T4	0.35	0.13	2.28	3.72	0.02	4.12
T5	0.35	0.13	2.28	3.71	0.02	4.12
Current, If	0.00	0.00	12.76	20.37	0.00	11.62

1.1.5.5 Simulation of Case ID24: grid current feedback (§1.5.3.4)

The harmonic compensation using grid current feedback as described in §1.5.3.4 has been implemented and validated through RSCAD simulations. The method is able to bring down the harmonic voltage levels at the 400 kV bus to the background levels as shown in Table XII. The grid side currents and the compensating currents for the STATCOM connected at the 220 kV bus T2 is shown in Fig. 25.

The compensation can be improved by using lead-lag filter in the feedback grid current. Thus, the compensating current can be decreased from 6.71% 4.46% to 5.04% and 3.37% respectively for compensation of the the 11th and the 13th harmonic respectively in the case ID #24.

Table XII. Case ID 24: Harmonic voltages at different busses and the STATCOM currents using grid current feedback for the 11th, 13, and the 19th harmonic orders.

Harmonic	5th	7th	11th	13th	17th	19th
Background	0.50	0.34	0.44	0.49	0.10	0.42
T1	0.22	0.23	0.44	0.49	0.1	0.42
T2	0.22	0.054	0.43	0.48	0.023	0.44
T3	0.34	0.12	0.81	0.55	0.015	0.24
T4	0.35	0.13	0.96	0.69	0.021	0.38
T5	0.35	0.13	0.96	0.69	0.021	0.38
Current, If	0.13	0.07	4.9	3.25	0.02	0.73

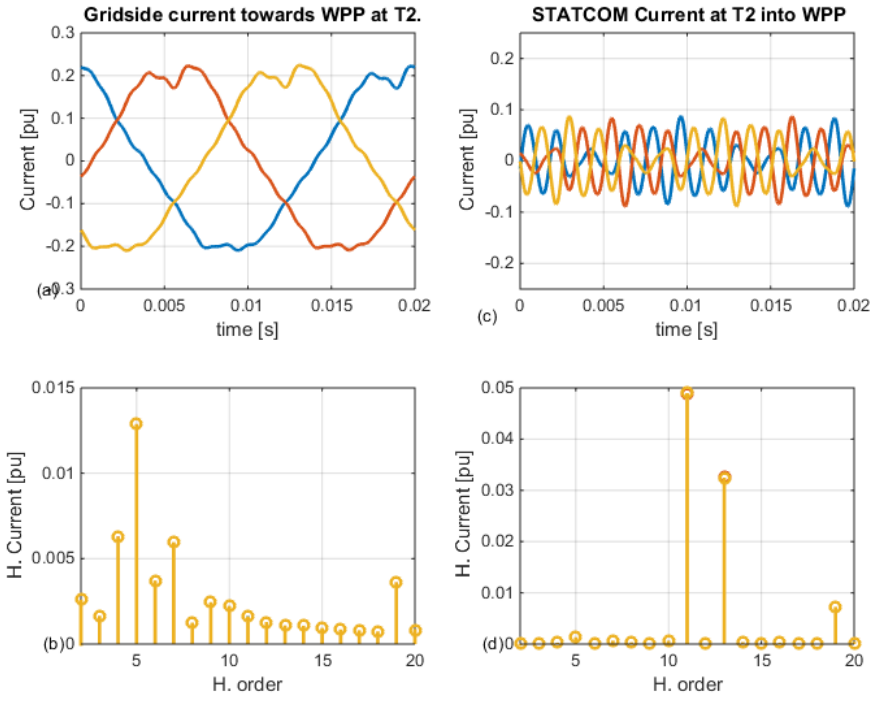

Fig. 25. Compensation using grid current feedback (a) Grid side currents. (b) Harmonic spectrum of grid side currents. (c) STATCOM currents. (d) Harmonic spectrum of STATCOM currents for $k_{11} = k_{13} = 30,\ \&\ k_{19} = 2$.

1.1.5.6 Transient simulation of Case ID24 with complex feedback of voltage from T1 (§1.5.3.1)

A series of switching transient events were created to observe the controller performance and stability against the transient events. Also since some network component gets switched off or on, this also indicates the robustness against some of the parameters to some extent. The following events were simulated in sequence with random time interval between them.

A. Start simulation with everything connected

B. Turn on the compensator

C. Switch off one of the two 410/233 kV transformers

D. Switch off one of the three collector-bus transformers

E. Switch off the second collector-bus transformers

F. Switch off half of the collector feeder connected to the remaining transformer

G. Switch on one of the two 410/233 kV transformers

It was observed that the switching on/off of the 410/233 kV transformer had maximum impact upon the harmonic voltage distortion at T1. Nevertheless, the compensator worked to mitigate the disturbance and drive the harmonic voltage levels to the reference limit levels as shown in Fig. 26. Other events like switching off/on the collector bus transformer, and the collector feeders had negligible impact.

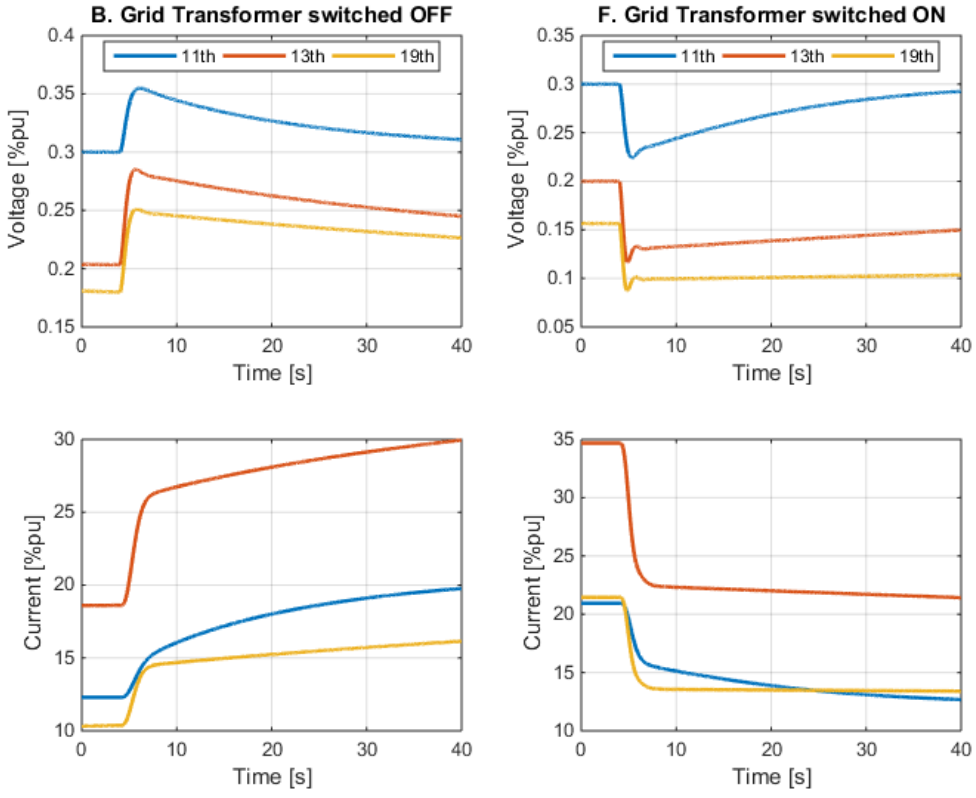

Fig. 26. Performance of the harmonic compensator during transformer switching transients.

1.1.5.7 Transient simulation of grid current feedback (§1.5.3.4)

The transient events listed in §1.1.5.6 were applied for the 16 cases with different values of grid impedances. All the cases were find to be stable. Further, very fast stabilization of the transients were observed after each of the switching events. The fast stabilization can be attributed to the fact that the voltage harmonics at T1 settles to the background harmonic levels, unlike very low harmonic voltage levels specified in the previous section (§1.1.5.6).

1.6. Utilization of project results

How do the project participants expect to utilize the results obtained in the project? Do any of the project participants expect to utilize the project results - commercially or otherwise? Which commercial activities and marketing results do you plan for? Has your business plan been updated? Or a new business plan produced? What future context is the end results expected to be part of, e.g. as part of another product, as the main product or as part of further development and demonstration? What is the market potential/Competition?

The project was exploring application of active filter functionality embedded in STATCOMs used in wind power plants. The outcome of the project led to significant increase of in-house knowledge regarding advantages and challenges of active filtering. Furthermore during the research project execution the first deliverables contributed to simultaneous first large-scale demonstration of active filtering embedded in STATCOMs in a commercial large offshore wind power plant. The demonstration, as well as the research project, appeared to be very successful and opened next gates to commercial application of this technology in future commercial projects.

Do project participants expect to take out patents?

The project participants do not expect to file any patent applications.

How do project results contribute to realize energy policy objectives?

The application of active filtering embedded in STATCOMs, especially in large offshore wind power plants where STATCOMs are typically needed to fulfill demanding grid code requirement, can potentially minimize development, capital and operating expenditures by reducing the state-of-the-art passive filter size or completely removing the need for it, and consequently reducing the cost of renewable electricity.

Have results been transferred to other institutions after project completion? If Ph.D.s has been part of the project, it must be described how the results from the project are used in teaching and other dissemination activities

Within the project a number of publications were released as a part of dissemination of knowledge. They were used in communication with various internal and external stakeholders in order to bring closer the concept of active filtering in wind power plants and initiate first steps in commercial application supporting demonstration activities and tendering processes.

1.7. Project conclusion and perspective

- Test grid model based on Anhiolt WPP has been developed in DigSILENT, PSCAD and RSCAD. Harmonic impedance scan and powerflow analysis analyses show similar behaviour in the three models, though there are differences.

- 24 Different grid impedance cases has been modelled in the form of frequency dependent network equivalent using vector curve fitting and modelled in PSCAD and RSCAD.

- Resistive compensation at the 400 kV and 220 kV bus nearest to the onshore grid has been analysed. It is concluded that such a compensation reduces the harmonic voltage distortion at the local bus and downstream. The reduction is not guaranteed on the upstream busses, there some cases there can be an amplification.

- Four new methods for harmonic compensation have been proposed and two of them have been investigated and validated through time domain simulations in PSCAD and RSCAD. One of them is based upon voltage feedback, while the other one is based upon current feedback.

- It has been demonstrated that the harmonic amplification at the remote 400 kV bus can be limited to the background harmonic levels by providing compensation at the 220 kV bus.

- Moreover, it is possible to attenuate the harmonic voltages at the 400 kV bus to levels lower than the background levels by providing compensation at the 220 kV bus. However, it increases the harmonic levels inside the WPP.

- Dynamic simulation of the controller in the presence of switching events of the grid transformer as well as the collector bus transformers has been carried out to confirm the robustness of the controller.

Annex

Summary of the simulation results of the 16 different case (Grid impedance case ID#1 to 24 except the cases 6, 13, and 18 to 23)

A. Harmonic compensation method using T1 voltage feedback (§1.1.5.2), and the feedback being complex transfer function.

B. Comparison of results with the complex (i.e. transfer function as described in (§1.1.5.2) and real (i.e. proportional as described in §1.1.5.4) feedback of voltage at T1.

C. Harmonic compensation method using real (proportional) feedback of grid current (§1.5.3.4)